MICROENCAPSULATION OF *SALVIA OFFICINALIS* L. ESSENTIAL OIL BY COMPLEX COACERVATION TECHNOLOGY

István SZÉKELY-SZENTMIKLÓSI[a], **Emőke Margit RÉDAI[b]**,
Robert-Alexandru VLAD[b], **Zoltán SZABÓ[a]**, **Béla KOVÁCS[c]**,
Attila-Levente GERGELY[d], **Csilla ALBERT[e]**,
Blanka SZÉKELY-SZENTMIKLÓSI[f*], **Emese SIPOS[a]**

ABSTRACT. The essential oil of *Salvia officinalis* L. (sage) exhibits versatile biological properties. The high sensitivity of sage essential oil (SEO) to environmental conditions and limited processability represent important hurdles in its use, which, however, can be overcome by microencapsulation. The objective of the current study was to encapsulate sage essential oil into core-shell type microcapsules by complex coacervation technology and to transform it into solid form by freeze-drying. Arabic gum (GA) and three different type A gelatin (G)

a   *George Emil Palade University of Medicine, Pharmacy, Science, and Technology of Targu Mures, Faculty of Pharmacy, Department of Pharmaceutical Industry and Management, 38 Gheorghe Marinescu str., RO-540142, Targu Mures, Romania*

b   *George Emil Palade University of Medicine, Pharmacy, Science, and Technology of Targu Mures, Faculty of Pharmacy, Department of Specialty Pharmaceutical Sciences, Pharmaceutical Technology, 38 Gheorghe Marinescu str., RO-540142, Targu Mures, Romania*

c   *George Emil Palade University of Medicine, Pharmacy, Science, and Technology of Targu Mures, Faculty of Pharmacy, Department of Fundamental Pharmaceutical Sciences, Pharmaceutical Biochemistry and the Chemistry of Environmental Factors, 38 Gheorghe Marinescu str., RO-540142, Targu Mures, Romania*

d   *Faculty of Economics, Socio-Human Sciences and Engineering, Sapientia Hungarian University of Transylvania, Department of Mechanical Engineering,1 Piața Libertății str. 530104 Miercurea Ciuc, Romania*

e   *Faculty of Economics, Socio-Human Sciences and Engineering, Sapientia Hungarian University of Transylvania, Department of Food Science,1 Piața Libertății, RO-530104 Miercurea Ciuc, Romania*

f   *George Emil Palade University of Medicine, Pharmacy, Science, and Technology of Targu Mures, Faculty of Pharmacy, Department of Specialty Pharmaceutical Sciences, Pharmaceutical Chemistry, 38 Gheorghe Marinescu str., RO-540142, Targu Mures, Romania*

*   *Corresponding author: blanka.szekely-szentmiklosi@umfst.ro*

grades were used to investigate the effect of the gel strength on microcapsule characteristics. The formation of essential oil containing microcapsules during complex coacervation was assessed by optical microscopy while SEM imaging was used to determine the morphology of the freeze-dried forms. Characterization of microcapsules was completed with FT-IR spectroscopy. Encapsulation efficiency was determined by UV-VIS spectrophotometry and the composition of essential oil by GC-MS technique. Results revealed that by the application of selected microencapsulation technology and freeze-drying method high encapsulation efficiency values could be achieved, the gel strength of gelatin has a decisive role in microcapsule particle size and the composition of essential oil is well preserved following the technological process.

INTRODUCTION

Sage (*Salvia officinalis* L., Figure 1) is a perennial evergreen subshrub, part of the Lamiaceae family. It is a well-known medicinal plant worldwide, which has been used since ancient times in traditional medicine. According to the European Union herbal monograph on *Salvia officinalis* L. - folium the well-established use could be considered as scientifically proven in mild dyspeptic complaints such as heartburn and bloating, relief of excessive sweating, inflammation in the mouth or the throat and minor skin inflammations [1,2]. But as the Latin name of the plant suggests (salvare = to save) and taking into account the extensive empirical experience, its healing effects might go beyond what has been proven so far which is still awaiting scientific confirmation.

Figure 1. Different development stages of sage (*Salvia officinalis* L.)

The major constituents of the essential oil are the terpenoids which are volatile and thermolabile in nature, prone to oxidation or hydrolysis depending on the structure. Thus, processing and storage conditions of plant material in the course of the extraction process and handling of obtained essential oil could greatly influence their chemical composition. On the other hand, the aging process of essential oils might be accompanied by the appearance of unpleasant flavors, a change of color or consistency, and even resinification. On the basis of these modifications could be oxidative damage, chemical transformations, or polymerization reactions [3].

The ISO standard 9909:1997 establishes the following acceptance criteria according to the chromatographic profile for compounds as presented in Figure 2 [4].
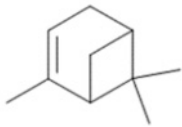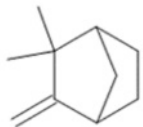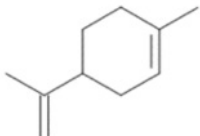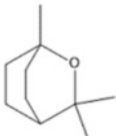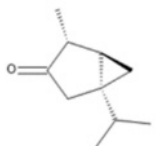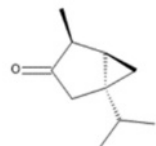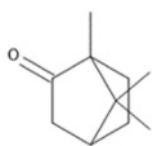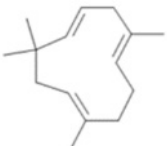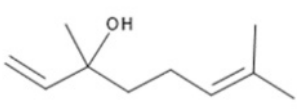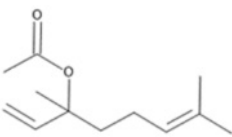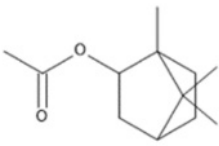

Figure 2. Controlled components of *Salvia officinalis* L. essential oil and their acceptance criteria according to ISO standard 9909:1997

Apart from compounds listed in the ISO standard, the composition of Sage essential oil is more complex and depending on cultivar, soil type, pedoclimatic conditions, and harvesting period as well as post-harvest management might have a specific fingerprint [5].

Given the sensibility of several components of essential oil to the effect of environmental conditions [3] proper formulation and conditioning is required to prevent degradation and assure long-term preservation of the particular composition [6]. In many cases, the transformation of essential oil from a liquid state into free-flowing and easily manageable dry powders might be of fundamental importance to fit a specific application [7].

Microencapsulation is one of the most widely used techniques for these purposes. Although numerous microencapsulation techniques have been developed since then, due to its simplicity and cost-effectiveness, complex coacervation remained one of the most widely applied methods in the food and pharmaceutical industry [8].

The production process of core-shell type microcapsules by complex coacervation is composed of the following basic steps: dissolution of polymers, emulsification of essential oil, coacervation, gelation, hardening, rinsing, separation of microcapsules, and drying. The phenomenon takes place in a narrow pH range, between the pKa of anionic polysaccharide and the isoelectric point of the protein [9]. Due to its advantageous properties such as biodegradability, low immunogenicity, easy availability, and low cost, gelatin (G) remained one of the most widely applied shell components for microencapsulation. Besides its widespread utilization in the food sector, it is present also in the pharmaceutical industry not only in the composition of solid, semi-solid, and liquid dosage forms but also in the development of nano- and microscale carrier systems as well as in tissue engineering and regenerative medicine [10].

The current study intends to investigate the possibility of applying complex coacervation technology to encapsulate SEO by assessing the effect of three different gelatin grades and obtaining solid form material by freeze-drying for possible further processing and to evaluate the effect of microencapsulation on the composition of the essential oil.

RESULTS AND DISCUSSION

Microscopic investigation of complex coacervate formation

According to the optical microscopic investigation, microcapsules were successfully obtained in the case of each gelatin grade applied. The impact of gel strength on the particle size of microcapsules could be observed.
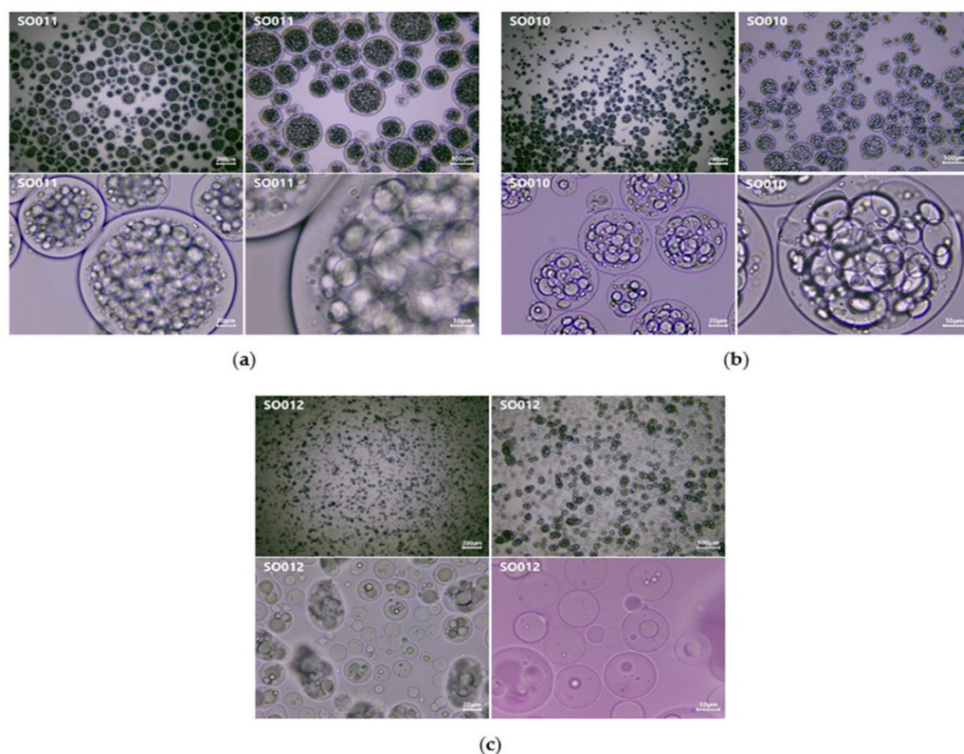
Figure 3. Optical microscopic images of formed microcapsules at 40X, 100X, 400X, and 1000X magnifications: (a) experiment no. SO011 manufactured with GE ≈300 Bloom; (b) experiment no. SO010 manufactured with GE ≈175 Bloom; (c) experiment no. SO012 manufactured with GE 80-120 Bloom;

According to the optical microscopic images (Figure 3), spherical microcapsules were formed at each experiment. The largest particles resulted in the case of experiment no. SO011 when gelatin grade with the highest gel strength (≈ 300 Bloom) was used. Contrarily, the smallest particles were formed in the case of microcapsules manufactured with gelatin grade having the lowest gel strength value of 80 – 120 Bloom (exp. no. SO012). Our results are in good alignment with conclusions drawn by Peters et al. during their study on the microencapsulation of theobromine that the diameter of microcapsules increased with increasing Bloom grade for type A gelatins [11]. Liu et al. tested five different grades of type B gelatins (140 Bloom, 180 Bloom, 200 Bloom, 220 Bloom, and 240 Bloom) in the complex coacervation of cinnamaldehyde with sodium carboxymethylcellulose. The authors found that the application of gelatin with 200 Bloom value resulted in microcapsules with the most uniform particle sizes [12].

225

I.SZÉKELY-SZENTMIKLÓSI, E. M. RÉDAI, R.-A. VLAD, Z. SZABÓ, B. KOVÁCS,
A.-L. GERGELY, CS. ALBERT, B. SZÉKELY-SZENTMIKLÓSI, E. SIPOS

Particle size measurements performed by optical microscopy for the three experimental runs are presented in Table 1, as follows:

Table 1. Particle size characteristics of microcapsules containing SEO manufactured with different gelatin grades

Exp. no.	Particle size (µm)			SD	RSD %	Median (µm)	Polydispersity index
	Average	Min.	Max.				
SO010	[1]55	16.2	135.3	23.85	43.31	52.60	0.19
SO011	[2]119	43.0	227.7	40.85	34.29	116.95	0.12
SO012	[3]25	8.2	93.3	10.58	42.80	23.90	0.18

[1] n = 826; [2] n = 340; [3] n = 903

The histograms of particle size distribution according to the microscopic measurements are presented in Figure 4.
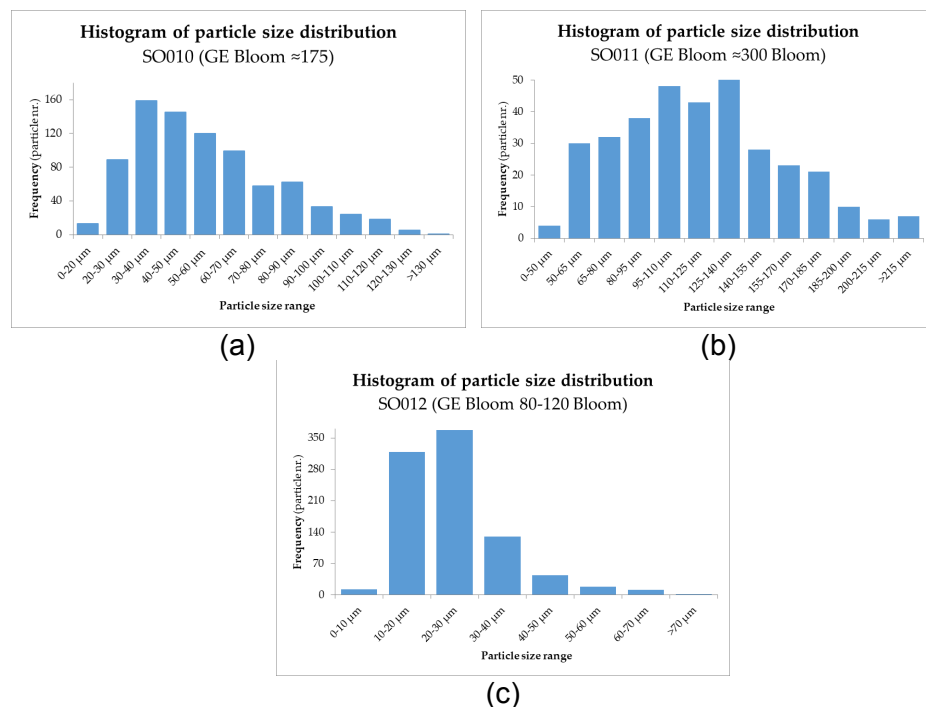

(a)

(b)

(c)

Figure 4. Histogram of particle size distribution of SEO microcapsules
(a) exp. no. SO010 with G≈175 Bloom; (b) exp. no. SO011 with G≈300 Bloom;
(c) exp. no. SO012 with G=80-120 Bloom.

The histograms for experiment no. SO010 and SO011 manufactured with medium and high gel strength G grades exhibit a bimodal distribution tendency with peaks in the particle size ranges of 30-40 µm, 80-90 µm and 95-110 µm, 125-140 µm respectively. In the case of experimental run SO013 incorporating G 80-120 Bloom the vast majority of microcapsules are concentrated between 10-40 µm.

In the case of the application of GA and G in a 1:1 ratio with gelatin type A with 175 Bloom gel strength, Rousi et al.[13] also reported a bimodal distribution and particle sizes somewhat lower in comparison to values obtained in the case of our experiment (SO010) incorporating G with the same Bloom value. Yang et al. [14] reported particle size values ranging from 5 to 12 µm when gelatin with 100 Bloom was used. Literature data suggest that besides gel strength another decisive factor in microcapsule particle size in the case of G-GA systems is the ratio between the two polymers.

On the microscopic images captured at smaller magnifications (40X, 100X) the high polydisperity grade could be observed which is a characteristic of complex coacervation technique. At higher magnifications (400X, 1000X) the polynucleated nature of the microcapsule core is clearly visible in the case of experimental runs containing gelatin grades with intermediate (exp. no. SO010) respective high (exp. no. SO011) gel strength values. In this respect, presumably due to the relation of emulsion droplet size and microcapsule dimensions, in the case of experiment no. SO012 resulting smallest particle sizes, mono- and oligonucleated microcapsules were also present in a large amount.

Assessment of freeze-dried microcapsules

- ### Macroscopic aspect of freeze-dried form

The effect of using different gelatin type A grades was reflected in the appearance of the lyophilized forms. Samples obtained by the application of gelatin with intermediate and high Bloom values (exp. no. SO010 and exp. no SO011) resulted in a lyophilized material with a looser structure and granular aspect. In case of exp. no. SO012 incorporating gelatin with low gel strength a more compact freeze-dried material was formed. (Figure 5)

Figure 5. Macroscopic aspect of the lyophilized samples obtained with different gelatin grades (exp. no. SO010 – G ≈175 Bloom; exp. no. SO011 – G ≈300 Bloom; exp. no. SO012 – G 80-120 Bloom).

• **Investigation of morphology by SEM**

SEM images were recorded for the freeze-dried form of the three experimental runs. The particle size differences observed by optical microscopy in correlation with gelatin grades are well reflected on the SEM images as presented in Figure 6.
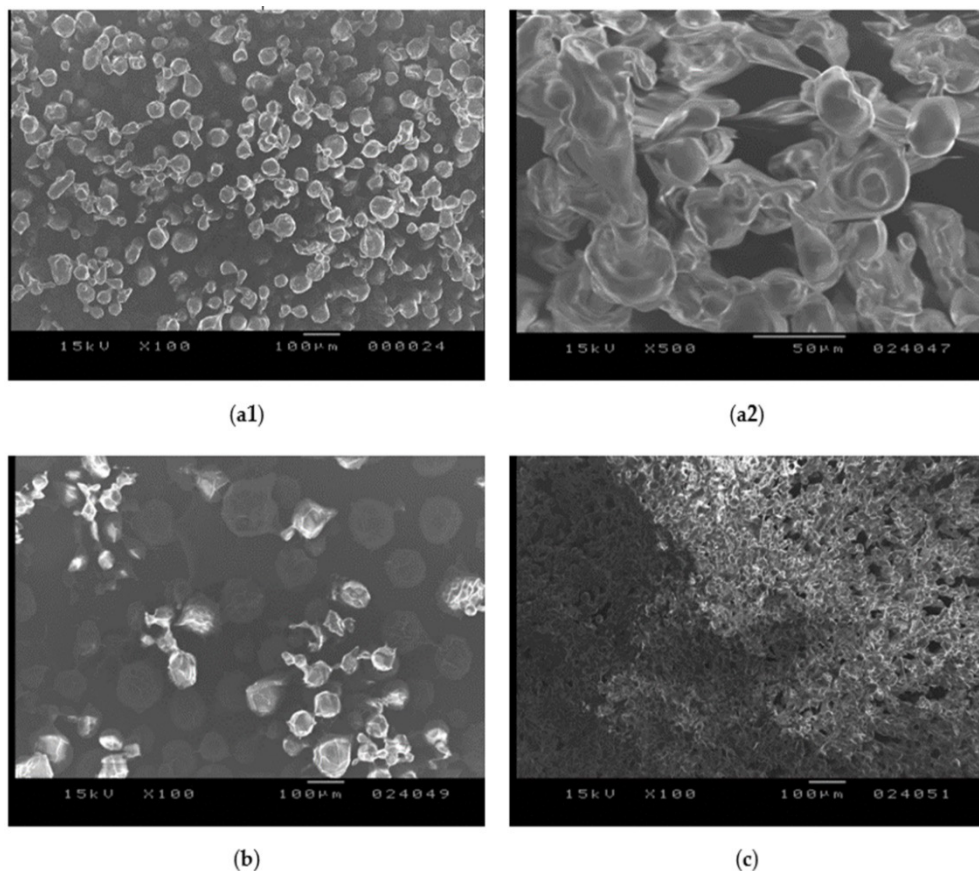

(a1)

(a2)

(b)

(c)

Figure 6. SEM images of freeze-dried microcapsules prepared with different gelatin grades: (a1) experiment no. SO010 manufactured with G ≈175 Bloom at 100X magnification and (a2) 500X magnification; (b) experiment no. SO011 manufactured with G ≈300 Bloom; (c) experiment no. SO012 manufactured G 80 - 120 Bloom.

The SEM images confirmed that the lower the gel strength of the G grade used, the smaller the resulting freeze-dried microcapsules are. A net-like structure is observed, which becomes denser as the particle size decreases. In experiment no. SO011, where gelatin with 300 Bloom gel strength was used, the individual spherical particles can be well distinguished with a specific wrinkled surface and only a few interconnections (Figure 6 - b). The application of gelatin with intermediate gel strength (175 Bloom – experiment no. SO010) resulted in the formation of a more interconnected structure, though the embedded spherical microcapsules remain easily distinguishable (Figure 6 – a1, a2). In experiment no. SO012 prepared with gelatin having the lowest gel strength, presumably due to the small size of formed microcapsules and associated high specific surface area, which facilitates the formation of interconnections, a denser, sponge-like structure was formed. In this case, individual microcapsules are hard to distinguish in the matrix that permeates the entire structure. Similar structures with interconnected particles following microencapsulation and subsequent freeze-drying were described by other authors [15–19].

The rehydration of lyophilized microcapsules could be easily performed. Upon the addition of water, the microcapsules regained almost instantly their original appearance (Figure 7). Our observation is in good alignment with that reported by Comunian et al. who described a similar phenomenon [20].
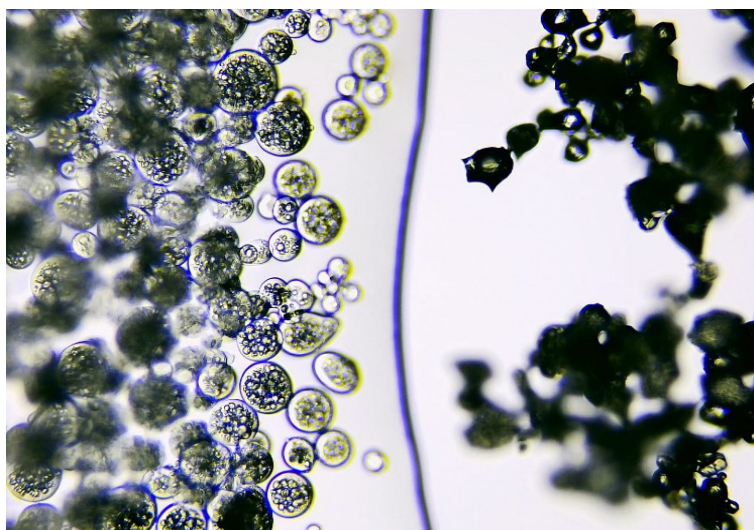

Figure 7. Lyophilized - (right) and rehydrated (left) microcapsules with water droplet propagation line in the middle captured by optical microscope for experiment no. SO010.

I.SZÉKELY-SZENTMIKLÓSI, E. M. RÉDAI, R.-A. VLAD, Z. SZABÓ, B. KOVÁCS,
A.-L. GERGELY, CS. ALBERT, B. SZÉKELY-SZENTMIKLÓSI, E. SIPOS

GC-MS investigation of essential oil composition

Table 2 contains the GC-MS results obtained for free essential oil as well as the SEO composition obtained from the microcapsules.

Table 2. GC-MS results of free- and microencapsulated SEO. (exp. no. SO010 - with G Bloom approx. 175, exp. no. SO011 – with G Bloom approx. 300, exp. no. SO012 – with G 80-120 Bloom)

Nr.	Compound*	SEO	SO010	SO011	SO012
		peak, %			
1	alpha pinene**	2.31	3.62	2.74	3.15
2	3-hexanol	-	1.00	-	-
3	camphene**	3.40	4.37	3.12	3.58
4	beta-pinene	1.63	1.84	1.25	1.41
5	beta myrcene	0.56	-	-	-
6	p-cymene	0.93	0.48	-	-
7	limonene**	1.64	1.29	0.83	0.89
8	1,8 cineole**	10.34	5.48	3.05	2.39
9	gamma terpinene	1.17	0.99	0.77	0.87
10	terpinolene	0.60	0.45	-	-
11	linalool**	-	-	1.19	0.83
12	alpha-thujone**	23.76	19.30	24.29	22.66
13	beta-thujone**	5.45	3.88	6.79	6.59
14	camphor**	19.78	12.90	12.21	11.82
15	endo borneol	4.99	3.26	4.86	4.87
16	terpinen-4-ol	0.72	0.43	-	-
17	linalyl acetate**	-	-	0.99	-
18	bornyl acetate	2.53	2.19	4.65	5.09
19	caryophyllene	8.65	9.11	14.82	15.86
20	isocaryophyllene	-	0.71	-	-
21	humulene**	9.18	11.92	17.04	17.96
22	caryophyllene oxide	0.25	-	-	-
23	viridiflorol	0.78	1.58	1.4	2.02
	Total identified	**98.67**	**84.80**	**100.00**	**99.99**

*In the order or retention times, ** Components controlled by the ISO standard.

Commercial SEO purchased from the Romanian market fulfilled the requirements of ISO standards for the quantitative composition. 19 compounds were identified in the free essential oil. The order of the five major components was: alpha thujone > camphor > 1,8-cineole > humulene > caryophyllene. Similar results for Salvia officinalis L. essential oil composition were reported by Baj et al. [21].

A general conclusion is that the composition of SEO was well preserved following microencapsulation in the case of each experimental run, although the amount of 1,8 cineole and camphor encountered a significant decrease, while the relative ratio of some components with lower volatility (higher molecular mass and lower boiling point), as it is the case of caryophyllene and humulene, increased. Caryophyllene oxide and beta-myrcene, present already in the lowest amounts in the composition of the free SEO could not be detected in either of the microcapsules. However, other two highly volatile compounds (p-cymene and terpinolene: an aromatic monoterpene and an alkene monoterpene) were retained in the composition of SO010. The appearance of 3-hexanol (SO010), linalool (SO011 and SO012), linalyl acetate (SO011), and isocaryophyllene (SO010) might be explained by their relative increase in the composition due to the loss of high volatile components during the technological process. It should be emphasized that in the case of experiment no. SO010 the same five major components were present in the composition of the encapsulated essential oil in the order of alpha thujone > camphor > humulene > caryophyllene > 1,8-cineole. In the case of experiments SO011 and SO012, the order of the five major components was: alpha thujone > humulene > caryophyllene > camphor > beta thujone.

Determination of encapsulation efficiency and loading capacity by UV spectroscopy

To determine the encapsulation efficiency, UV-visible spectroscopic measurements were undertaken at the absorption maximum of sage essential oil in ethanol, at wavelength 241 nm, and concentrations were determined by interpolation of the absorption of sage essential oil from microcapsules to a previously constructed calibration curve in ethanol. The blank microcapsules (PL) showed no absorption in this region, indicating that the presence of oil can be detected in the microcapsule solutions.

The calibration diagram was constructed using the concentrations and measured absorbances of six different alcoholic solutions of SEO, ranging from 25-65 µg/ml. The resulting equation, y = 0.0522 X – 0.0079 with $R^2 = 0.991$, demonstrates a high linear correlation between SEO concentrations and absorbances at 241 nm.

The encapsulation efficiency (EE) and loading capacity (LC) are presented in Table 3 and should be taken into consideration to determine the efficiency of the microencapsulation process. A similar spectrophotometric method with the application of ethanol was applied by Gonçalves et al [22].

Table 3. Encapsulation efficiency and loading capacity for SEO microcapsules.

Sage essential oil in microcapsules SO010	SEO concentration (µg/ml)[1]	Concentration of microcapsule solution (µg/ml)	Theoretical (initial) oil content (µg/ml)	EE %	LC%
Total oil content	39.36	100	40.29	86.00	34.65
Surface oil content	4.71	100	40.29		

[1] *Calculated based on the straight-line equation and the measured absorbance values.*

Encapsulation efficiency refers to the proportion of core material successfully trapped within the microcapsules, serving as an important index for assessing the efficiency of microencapsulation [23,24].

Loading capacity, on the other hand, measures the amount of encapsulated core material relative to the total mass of the microcapsule.

Due to the limited literature available on the microencapsulation of sage essential oil, the results were compared with the encapsulation of other substances and essential oils in a G-GA system, using similar parameters. For example, Xiao-Ying Qv et al. achieved an EE of 85-86 % when encapsulating lutein [25], while Glaucia A. Rocha-Selmi et al. reported EE values above 90% for lycopene microcapsules [26]. Ferreira S. and Nicoletti V.R. found EE values ranging from 89.7 to 98.7% for a ginger oil formulation prepared with the method of complex coacervation [27]. In a full factorial experimental design, Rungwasantisuk and Raibhu obtained EE values in the range of 67 - 85 % for complex coacervate of lavender oil using type A gelatin with 170-175 Bloom, gum arabic and glutaraldehyde as crosslinker, with freeze-drying [28]. Burhan et al. achieved a maximum EE of 77.9% for lavender oil microencapsules prepared with GA and maltodextrin, using spray drying. They applied also a UV-VIS spectrophotometric method for determination, the essential oil being extracted with 5 w/v% sodium lauryl sulfate solution [29]. Zhang et al. emphasized that the type and composition of wall materials, along with the drying process significantly influence EE values, which are typically high when gelatin is used alongside GA and sodium caseinate in complex coacervation [23]. Xiao et al. suggested that some essential oil loss might occur due to volatilization during emulsification and coacervation at around 50°C [30]. However, according to Napiórkowska et al., the type of oil has only a minor impact on EE [31].

The EE value obtained in our experiment is relatively high and aligns well with those reported in the literature for complex coacervation.

As for loading capacities, various ranges have been reported in the literature, attributed to differences in core materials, macromolecule types, and wall material ratios. Calderón-Oliver et al. reported the loading capacity of nisin and avocado peel extract ranging from 3.05 to 13.59 % and 4.58 to 20.54%, respectively [32], while the LC of coacervated black raspberry anthocyanin microcapsules prepared by Shaddel et al. ranged from 29.67 to 38 % [33].

FT-IR spectroscopy

Figure 8 shows the FT-IR spectrum of the microcapsule from experiment SO010, compared with the spectra of the shell (PL) and core (SEO), as well as the spectra of the shell material components, namely 175-Bloom gelatin (GE) and gum arabic (GA).
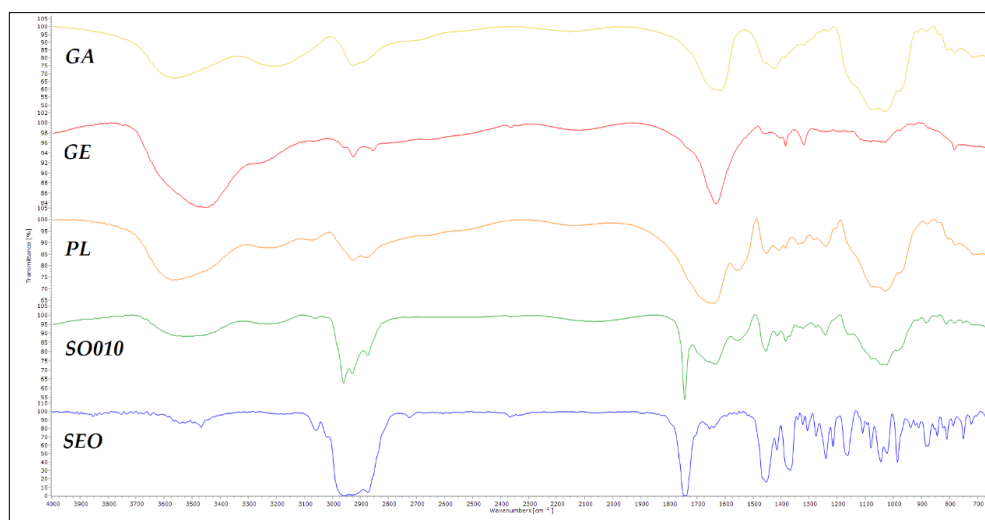
Figure 8. The FT-IR spectra of gum arabic (GA), gelatin (GE), oil-free microcapsule (PL), microcapsules (SO010), and essential oil (SEO)

The FT-IR spectrum of gelatin polypeptide displays a broad peak at 3453 cm^{-1}, and a smaller peak at 3225 cm^{-1}, reflecting N-H stretching of amide bonds and –NH$_2$ groups, as well as O-H stretching vibrations from hydroxyl groups in amino acid side chains [14,19]. The peak at 2924 cm^{-1} is

due to the stretching vibrations of C-H bonds, while the peak at 1385 cm^{-1} is associated with the bending vibrations of C-H bonds in the aliphatic chains of amino acid residues. A prominent peak at 1632 cm^{-1} arises from C=O stretching vibrations in amide bonds in the polypeptide backbone, while the peak at 1032 cm^{-1} indicates C-N stretching vibrations of amine groups or C-O stretching of hydroxyl groups [13,34].

Gum arabic is a complex mixture of polysaccharides and glycoproteins [35]. Its FT-IR spectrum (Figure 8) shows a strong absorption band at 3567 cm^{-1}, due to the –OH stretching vibrations of free or hydrogen-bonded hydroxyl groups in polysaccharides, and a peak at 3212 cm^{-1} linked to N-H stretching from glycoproteins [13]. The weaker peak at 2925 cm^{-1} suggests C-H stretching vibrations in alkyl groups indicating hydrocarbon chains within the polysaccharides. Peaks at 1617 cm^{-1} and 1425 cm^{-1} correspond to carboxylate groups' (–COO-) asymmetrical and symmetrical stretching vibrations [31] mainly from glucuronic acid units, while the strong absorption band at 1031 cm^{-1} indicates asymmetric stretching vibration of –C-O-C and –C-O in glycosidic linkages and hydroxyl groups in polysaccharides [34,36].

The FT-IR spectrum of SEO contains various peaks corresponding to the different functional groups present in its chemical constituents. It has a broad peak likely resulting from the overlap of three distinct peaks at 2958 cm^{-1}, 2935 cm^{-1}, and 2871 cm^{-1}, corresponding to C-H stretching vibrations of methyl (-CH$_3$) and methylene (-CH$_2$-) groups. The peak at 1742 cm^{-1} is indicative of a C=O stretching vibration of carbonyl groups, which could be due to the presence of ketones like thujone and camphor. The peaks at 1454 cm^{-1} and 1367 cm^{-1} can be attributed to C-H bending (scissoring) vibrations in -CH$_2$- groups, and C-H bending (deformation) vibrations of methyl groups (-CH$_3$), respectively, characteristic to isoprenoid compounds. The peaks corresponding to single-bonded oxygen-containing components are also present in the spectrum. For example, the peak at 1240 cm^{-1} due to C-O stretching vibrations indicates the presence of alcohols (e.g. linalool, borneol), esters (bornyl acetate), or ethers (1,8 cineole, caryophyllene oxide). Similarly, the peak at 1166 cm^{-1}, which corresponds to C-O-C stretching vibrations suggests the presence of ethers and esters. The peak at 1041 cm^{-1} related to C-O stretching vibrations is also characteristic of alcohols and ethers [37]. The peak at 980 cm^{-1} could be associated with =C-H bending vibrations of alkene groups or out-of-plane bending vibrations of aromatic C-H. This indicates the presence of unsaturated terpenes (e.g. pinene, humulene, limonene) and aromatic compounds (p-cymene) in sage essential oil [36].

During complex coacervation, at pH below its isoelectric point (pH≈4) the positively charged amino groups of G will react with oppositely charged carboxylic groups of GA polysaccharides by electrostatic interaction forming

polyionic complexes [38]. The FT-IR spectrum of the blank coacervates (PL) shows characteristic peaks of both G and GA at 3570 cm^{-1}, 2225 cm^{-1}, 2926 cm^{1}, and 1638 cm^{-1}. New peaks at 1240 cm^{-1} and 1029 cm^{-1} suggest N-H groups forming hydrogen bonds and participating in electrostatic interactions when protonated (NH_3^+), as well as C-O stretching in GA, indicating the involvement of carboxylate groups (COO-) in electrostatic interactions [13,34].

To investigate the interactions between the wall and the core materials, the FT-IR spectra of the SEO-containing microcapsules were compared with the spectrum of essential oil (Figure 8 SEO) and the spectrum of the blank microcapsules (Figure 8 PL). In the oil-containing microcapsules, the characteristic peaks of PL are present at wavelengths 3570 cm^{1} and 1638 cm^{1}, and the peak of SEO at 2958 cm^{-1}. Some peaks of PL overlap with those of SEO in the wavelength regions of 2926 cm^{-1} -2871 cm^{-1}, at 1240 cm^{-1}, and between 1030 cm^{-1} and 1040 cm^{-1}.

The unchanged essential oil peaks within the microcapsule matrix, along with the absence of new peaks, indicate that the SEO was successfully encapsulated without significant interaction with the wall materials, confirming that the encapsulation involved physical rather than chemical interactions [23,29,30].

CONCLUSIONS

Microencapsulation of SEO was successfully performed by the application of each G grade investigated using complex coacervation with GA along with glycerol as a crosslinker.

The particle size of SEO-containing microcapsules was determined by the gel strength of the G grade used. The incorporation of G with the highest Bloom value resulted in the largest particles, while the smallest microcapsules were obtained when G grade with the lowest gel strength was used. Average particle size values measured were 25 μm, 55 μm, and 119 μm, respectively. SEM investigation reflected the same trend regarding the correlation between gel strength and microcapsule particle size and revealed the net-like structure of lyophilized forms with different compactness.

According to the GC-MS analysis, the SEO composition was well preserved following the microencapsulation process. Most of the components identified in the free SEO were retained in the case of experimental run no. SO010 incorporating G with intermediate gel strength of approx. 175 Bloom where 17 compounds were identified out of 19 present in the free SEO.

EE determined by UV-VIS spectrophotometric method for experimental run proved to assure the best protection (SO010) was 86 %.

The FT-IR investigation confirmed that microcapsule shell formation is based on electrostatic interactions as the formation of new chemical bonds was not identified.

EXPERIMENTAL SECTION

Core material: Salvia officinalis L. essential oil – was purchased from the Romanian market

Shell materials: Gelatin type A of porcine origin 80-120 Bloom, approx. 175 Bloom and approx. 300 Bloom value were purchased from Sigma Aldrich (St. Louis, USA). Gum arabic (GA) from acacia tree was purchased from Sigma Aldrich Chemie (Steinheim, Germany).

pH adjustment: 0.5 N HCl was used for pH adjustment. Hydrochloric acid was purchased from Silal Trading SRL (Romania, Bucharest).

Crosslinker: Glycerol was purchased from Chimreactiv SRL (Romania, Bucharest)

Microencapsulation method: Complex coacervation technology was applied according to the following major steps: 50 g of 3% w/w GA aqueous solution was prepared by dissolving gum arabic at room temperature under continuous stirring by the means of a magnetic stirrer (Arec, Velp Scientifica, Europe) at 800 rpm. 50 g of 3% G aqueous solution was prepared under continuous stirring and concomitant heating up to $50 \pm 2°C$ using a magnetic stirrer at 800 rpm. Three different gelatin type A grades were used with gel strength values as follows: ≈ 175 Bloom (for experiment no. SO010), ≈ 300 Bloom (for experiment no. SO011), and ≈ 80 – 120 Bloom (for experiment no. SO012). In each case 2.7 g of Salvia officinalis essential oil was emulsified into the formerly prepared 3% w/w G solution by using an IKA DI 18 B type ultraturrax (IKA®-Werke GmbH & Co. KG, Staufen, Germany) equipped with an IKA S 18 N – 19 G type dispersion tool (IKA®-Werke GmbH & Co. KG, Staufen, Germany) for 10 minutes at rotation speed of ≈ 5,000 rpm. This emulsion was added to the formerly prepared aqueous gum arabic solution under continuous stirring at approx. 50°C. HCl 0.5 N solution was used to adjust the pH of the obtained mixture to pH=4.0 ± 0.05. After cooling to 10°C in an ice bath, the crosslinking agent glycerol (1 g) was added to harden the formed shell. Separation and purification of microcapsules were performed by decantation and washing with purified water (volume 3 x 50 mL): after decantation 50 mL of water was added to the microcapsule slurry and the mixture was stirred with a magnetic stirrer for 20 minutes. The washing procedure was repeated three times. Simultaneously, microcapsules without essential oil referred to as placebo were produced using the aforementioned method.

Freeze drying of microcapsules was performed in a Biobase BK FD10S (Biobase, Jinan, China) equipment by applying 4 hours of freezing at -55°C followed by 20 hours of drying under a vacuum of 10 Pa.

Optical microscopic investigation was performed on an Optika B-150D-BRPL (Optika SRL, Ponteranica, Italy) brightfield microscope equipped with an integrated 3.1 MP camera at magnifications of 40X, 100X, 400X, and 1000X. For particle size measurement Optika Proview software (Optika SRL, Ponteranica, Italy) was used. Microscopic specimens were prepared by bringing from the last washing cycle one droplet of microcapsule dispersion on a glass slide after which a cover slip was gently applied. In the case of the 1000X magnification immersion oil was applied on the top of the cover slip.

SEM investigation: the morphology of the obtained products was investigated by scanning electron microscopic (SEM) imaging, with the use of a JEOL JSM-5200 scanning electron microscope (JEOL, Tokyo, Japan) at 10 kV potential. The samples were used as is (without sputter coating) and were fixed by conductive carbon adhesive tape.

FT-IR spectroscopy of solid samples was performed on a Bruker Tensor 27 IR spectrophotometer (Bruker Optics, Ettlingen, Germany) controlled by the Opus software (version 7.2). IR spectra of the solid components, the physical mixture, and the prepared products were recorded using KBr (Sigma Aldrich, Merck, Darmstadt, Germany) pellets, in transmittance mode over 400 – 4000 cm-1 wavenumber range. The sample to KBr ratio was 1:100. Each sample was scanned 16 times, with a resolution of 2 cm^{-1}.

FT-IR spectroscopy of essential oil was performed on a Nicolet 380 IR spectrophotometer (Thermo Electron Corporation, Madison, USA) controlled by the OMNIC software.

UV-VIS spectroscopic determinations were performed on a Shimadzu UV-1800 spectrophotometer (Shimadzu Co., Kyoto, Japan), controlled by UVProbe Software, using cuvettes made of special quartz glass with an optical path length of 10 mm (Hellma Analytics, Müllheim, Germany).

SEO content in the microcapsules was determined by UV-VIS spectroscopic method and quantified through the calculation of encapsulation efficiency and loading capacity.

The amount of essential oil in the microcapsules was measured through the following steps: first, 10 mg of microcapsules were powdered in a mortar, and 100 mL of absolute alcohol was added. The mixture was magnetically stirred for 15 minutes, to dissolve the total quantity of essential oil. Then, another 10 mg of microcapsules were stirred with 100 mL alcohol for 15 minutes, and the supernatant was collected, to recover the SEO on the surface of the microcapsules. The alcoholic solutions were filtered and analyzed spectrophotometrically at 241 nm after appropriate dilution. SEO concentrations were determined using a calibration curve built within the range of 25-65 µg/ml.

The encapsulation efficiency (EE) and loading capacity (LC) were calculated using the following equations:

$$EE = \frac{m_m}{m_o} \times 100$$

where m_m represents the amount (mg) of oil contained in microcapsules, while m_o is the initial oil amount (mg) used. The amount of oil in microcapsules is determined by the difference between the total oil content (m_{to}) and the surface oil content (m_{so}):

$$m_m = m_{to} - m_{so}$$

$$LC = \frac{m_m}{M} \times 100$$

where M is the total amount (mg) of microcapsules.

GC–MS analysis of the essential oil was accomplished on an Agilent single-quadrupole mass spectrometer with an inert mass selective detector (MSD-5977 A, Agilent Technologies, USA). It was directly connected to an Agilent 7890B gas chromatograph with a split–splitless injector, a quick-swap assembly, an Agilent 7693 autosampler, and a HP-5MS fused silica capillary column (5% phenyl 95% dimethylpolysiloxane, 30 m × 0.25 mm internal diameter, 0.25 μm film thickness, Agilent Technologies, USA). The column was operated with an injector temperature of 250 °C. The oven temperature profile consisted of an isothermal hold at 50 °C for 4 minutes, a ramp of 4°C/min to 220°C, an isothermal hold for 2 minutes, followed by a second ramp to 280 °C at 20 °C/min, and a final isothermal hold for 15 minutes.

Before analysis, the essential oil was dissolved in hexane (1/100, v/v) and 1 μL of the solution was injected in 1:10 split mode. Extraction of essential oil from MC was performed from 250 mg freeze-dried material with 1 mL of hexane followed by filtration. As carrier gas helium was used at a flow rate of 1 ml/min. MSD ChemStation software, version F.01.01.2317 (Agilent) was used to obtain GC–TIC profiles and mass spectra. All mass spectra were acquired in the EI mode (scan range of m/z 45–600 and ionization energy of 70 eV). The electronic-impact ion source and the MS quadrupole temperatures were set at 230 °C and 150°C, respectively, with the MSD transfer line maintained at 280°C. For spectrum searching and identification NIST 14 MS spectrum library was used.

REFERENCES

1. Committee on Herbal Medicinal Products (HMPC); *EMA Salvia Monograph*, 2016, *44*.
2. Committee on Herbal Medicinal Products (HMPC); *Eur. Med. Agency - Comm. Herb. Med. Prod.*, 2016, *44*.
3. M. Jakovljević; S. Jokić; M. Molnar; M. Jašić; J. Babić; H. Jukić; I. Banjari; *Plants*, 2019, *8*, 55.
4. A. L. Lopresti; *Drugs R D*, 2017, *17*, 53–64.
5. G. P. Eckert; *Front. Pharmacol.*, 2010, *1*, 138.
6. M. Miroddi; M. Navarra; M. C. Quattropani; F. Calapai; S. Gangemi; G. Calapai; *CNS Neurosci. Ther.*, 2014, *20*, 485–495.
7. D. O. Kennedy; S. Pace; C. Haskell; E. J. Okello; A. Milne; A. B. Scholey; *Neuropsychopharmacology*, 2006, *31*, 845–852.
8. T. Hase; S. Shishido; S. Yamamoto; R. Yamashita; H. Nukima; S. Taira; T. Toyoda; K. Abe; T. Hamaguchi; K. Ono et al.; *Sci. Rep.*, 2019, *9*, 1–13.
9. S. Datta; S. Patil; *J. Alzheimer's Dis.*, 2020, *12*, 131–143.
10. S. K. El Euch; D. B. Hassine; S. Cazaux; N. Bouzouita; J. Bouajila; *South African J. Bot.*, 2019, *120*, 253–260.
11. R. Tundis; M. Leporini; M. Bonesi; S. Rovito; N. G. Passalacqua; *Molecules*, 2020, *25*, 5826.
12. R. Bleiziffer; C. Mesaros; S. Suvar; P. Podea; A. Iordache; F.-D. Yudin; M. Culea; *Stud. Univ. Babeş-Bolyai Chem.*, 2017, *62*, 373–385.
13. A. Russo; C. Formisano; D. Rigano; F. Senatore; S. Delfine; V. Cardile; S. Rosselli; M. Bruno; *Food Chem. Toxicol.*, 2013, *55*, 42–47.
14. S. Sertel; T. Eichhorn; P. K. Plinkert; T. Efferth; *HNO*, 2011, *59*, 1203–1208.
15. M. Yanagimichi; K. Nishino; A. Sakamoto; R. Kurodai; K. Kojima; N. Eto; H. Isoda; R. Ksouri; K. Irie; T. Kambe et al.; *Biochem. Biophys. Reports*, 2021, *25*, 100882.
16. H. A. Mohammed; H. M. Eldeeb; R. A. Khan; M. S. Al-Omar; S. A. A. Mohammed; M. S. M. Sajid; M. S. A. Aly; A. M. Ahmad; A. A. H. Abdellatif; S. Y. Eid et al.; *Molecules*, 2021, *26*, 5757.
17. C. Turek; F. C. Stintzing; *Compr. Rev. Food Sci. Food Saf.*, 2013, *12*, 40–53.
18. International Organization for Standardization; *Oil of Dalmatian Sage (Salvia Officinalis L.)*; Geneva, Switzerland, 1997; Vol. ISO 9909:1.
19. G. Tibaldi; S. Hazrati; S. J. Hosseini; A. Ertani; R. Bulgari; S. Nicola; *Ind. Crops Prod.*, 2022, *183*, 114923.
20. V. I. Sousa; J. F. Parente; J. F. Marques; M. A. Forte; C. J. Tavares; *Polymers (Basel)*, 2022, *14*, 1730.
21. M. Arenas-Jal; J. M. Suñé-Negre; E. García-Montoya; *Eur. Food Res. Technol.*, 2020, *246*, 1371–1382.
22. C. Thies; In *Encapsulation and Controlled Release Technologies in Food Systems*; J. M. Lakkis, Ed.; John Wiley & Sons Inc., 2016; pp. 41–77.

23. F. W. Tiebackx; *Zeitschrift für Chemie und Ind. der Kolloide*, 1911, *8*, 198–201.
24. G. O. Fanger; In *Microencapsulation*; Springer US: Boston, MA, 1974; pp. 1–20.
25. Y. P. Timilsena; T. O. Akanbi; N. Khalid; B. Adhikari; C. J. Barrow; *Int. J. Biol. Macromol.*, 2019, *121*, 1276–1286.
26. Z. Xiao; W. Liu; G. Zhu; R. Zhou; Y. Niu; *J. Sci. Food Agric.*, 2014, *94*, 1482–1494.
27. F. Milano; A. Masi; M. Madaghiele; A. Sannino; L. Salvatore; N. Gallo; *Pharmaceutics*, 2023, *15*, 1499.
28. C. E. Sing; S. L. Perry; *Soft Matter*, 2020, *16*, 2885–2914.
29. L. Zhou; H. Shi; Z. Li; C. He; *Macromol. Rapid Commun.*, 2020, *41*, 1–20.
30. H. J. W. Peters; E. M. G. van Bommel; J. G. F.; *Drug Dev. Ind. Pharm.*, 1992, *18*, 123–134.
31. B. Liu; L. Lai; B. Muhoza; S. Xia; *Food Biosci.*, 2021, *44*, 101403.
32. R. Shaddel; J. Hesari; S. Azadmard-Damirchi; H. Hamishehkar; B. Fathi-Achachlouei; Q. Huang; *Int. J. Biol. Macromol.*, 2018, *107*, 1800–1810.
33. I. D. Alvim; C. R. F. Grosso; *Ciência e Tecnol. Aliment.*, 2010, *30*, 1069–1076.
34. S. Leclercq; K. R. Harlander; G. A. Reineccius; *Flavour Fragr. J.*, 2009, *24*, 17–24.
35. A. S. Prata; M. H. A. Zanin; M. I. Ré; C. R. F. Grosso; *Colloids Surfaces B Biointerfaces*, 2008, *67*, 171–178.
36. A. S. Prata; C. R. F. Grosso; *J. Am. Oil Chem. Soc.*, 2015, *92*, 1063–1072.
37. Y. P. Lemos; P. H. Mariano Marfil; V. R. Nicoletti; *Int. J. Food Prop.*, 2017, *20*, 1–10.
38. B. Muhoza; S. Xia; J. Cai; X. Zhang; E. Duhoranimana; J. Su; *Food Hydrocoll.*, 2019, *87*, 712–722.
39. B. Muhoza; S. Xia; X. Zhang; *Food Hydrocoll.*, 2019, *97*, 105174.
40. Z. Rousi; C. Malhiac; D. G. Fatouros; A. Paraskevopoulou; *Food Hydrocoll.*, 2019, *96*, 577–588.
41. W. Yang; Y. Gong; Y. Wang; C. Wu; X. Zhang; J. Li; D. Wu; *RSC Adv.*, 2024, *14*, 4880–4889.
42. T. A. Comunian; J. Gomez-Estaca; R. Ferro-Furtado; G. J. A. Conceição; I. C. F. Moraes; I. A. De Castro; C. S. Favaro-Trindade; *Carbohydr. Polym.*, 2016, *150*, 319–329.
43. P. H. M. Marfil; B. B. Paulo; I. D. Alvim; V. R. Nicoletti; *J. Food Process Eng.*, 2018, *41*, 1–11.
44. G. A. Rocha-Selmi; F. T. Bozza; M. Thomazini; H. M. A. Bolini; C. S. Fávaro-Trindade; *Food Chem.*, 2013, *139*, 72–78.
45. M. G. Santos; F. T. Bozza; M. Thomazini; C. S. Favaro-Trindade; *Food Chem.*, 2015, *171*, 32–39.
46. T. A. Comunian; M. Thomazini; A. J. G. Alves; F. E. De Matos Junior; J. C. De Carvalho Balieiro; C. S. Favaro-Trindade; *Food Res. Int.*, 2013, *52*, 373–379.
47. T. Baj; A. Ludwiczuk; E. Sieniawska; K. Skalicka-Woźniak; J. Widelski; K. Zieba; K. Głowniak; *Acta Pol. Pharm.*, 2013, *70*, 35–40.
48. N. D. Gonçalves; C. R. F. Grosso; R. S. Rabelo; M. D. Hubinger; A. S. Prata; *Carbohydr. Polym.*, 2018, *196*, 427–432.

49. R. Zhang; L. Huang; X. Xiong; M. C. Qian; H. Ji; *Flavour Fragr. J.*, 2020, *35*, 157–166.
50. F. Baghi; S. Ghnimi; E. Dumas; A. Gharsallaoui; *Appl. Sci.*, 2023, *13*, 6184.
51. X.-Y. Qv; Z.-P. Zeng; J.-G. Jiang; *Food Hydrocoll.*, 2011, *25*, 1596–1603.
52. G. A. Rocha-Selmi; C. S. Favaro-Trindade; C. R. F. Grosso; *J. Chem.*, 2013, *2013*, 982603.
53. S. Ferreira; V. R. Nicoletti; *J. Food Eng.*, 2021, *291*, 110214.
54. A. Rungwasantisuk; S. Raibhu; *Prog. Org. Coatings*, 2020, *149*, 105924.
55. A. M. Burhan; S. M. Abdel-Hamid; M. E. Soliman; O. A. Sammour; *J. Microencapsul.*, 2019, *36*, 250–266.
56. Z. Xiao; W. Liu; G. Zhu; R. Zhou; Y. Niu; *Flavour Fragr. J.*, 2014, *29*, 166–172.
57. A. Napiórkowska; A. Szpicer; I. Wojtasik-Kalinowska; M. D. T. Perez; H. D. González; M. A. Kurek; *Foods*, 2023, *12*, 4345.
58. M. Calderón-Oliver; R. Pedroza-Islas; H. B. Escalona-Buendía; J. Pedraza-Chaverri; E. Ponce-Alquicira; *Food Hydrocoll.*, 2017, *62*, 49–57.
59. P. J. Larkin; *Infrared Raman Spectrosc.*, 2018, *85–134*.
60. H. H. Musa; A. A. Ahmed; T. H. Musa; In *Gum Arabic: Chemistry, Biological and Pharmacological Properties*; Springer, 2019; pp. 797–814.
61. B. H. Stuart; In *Infrared Spectroscopy: Fundamentals and Applications*; John Wiley & Sons Inc.: Hoboken, NJ, USA, 2004; pp. 71–80.
62. L. Ciko; A. Andoni; F. Ylli; E. Plaku; K. Taraj; A. Çomo; *Asian J. Chem.*, 2016, *28*, 1401–1402.
63. L. Ang; Y. Darwis; L. Por; M. Yam; *Pharmaceutics*, 2019, *11*, 451.